



An Analytical Procedure for Buckling Load Determination of an Axisymmetric Cylinder with Non-Uniform Thickness Using Shear Deformation Theory

F. Mahboubi Nasrekani, H. R. Eipakchi*

Faculty of Mechanical and Mechatronics Engineering, Shahrood University of Technology, Shahrood, Iran

ABSTRACT: In this article, the buckling load of an axisymmetric cylindrical shell with a variable thickness is determined analytically by using the perturbation method. The loading is axial and the material properties are defined by the Hooke's law. The displacement field is predicted by using the first order shear deformation theory and the nonlinear von-Karman relations are used for the kinematic description of the shell. The stability equations, which are the system of nonlinear differential equations with variable coefficients, are derived by the virtual work principle and are solved using the perturbation technique. Also, the buckling load is determined by using the finite element method and it is compared with the analytical solution results, the classical shell theory, and other references. The effects of linear and nonlinear shell profiles variation on the axial buckling load are investigated. Also, we studied the effects of geometric parameters on the buckling load results. The results show that the first order shear deformation theory is more useful for buckling load determination of thicker shells.

Review History:

Received: 26 February 2017
Revised: 5 July 2017
Accepted: 16 July 2017
Available Online: 21 October 2017

Keywords:

Buckling load
Cylindrical shell
Varying thickness
Shear deformation theory
Perturbation technique

1- Introduction

Buckling load determination of a shell with a variable thickness is interesting due to conserving the weight. Hutchinson [1] calculated the axial buckling load of a shell with initial geometric imperfection by using the Rayleigh-Ritz method. Morgan et al. [2] investigated the effects of R/h (radius to thickness ratio) on the buckling load of cylindrical and conical shells experimentally. Malik et al. [3] determined the buckling load of a cylindrical shell with a variable thickness under external pressure by using an experimental method. Mahboubi and Eipakchi [4] extracted the equations of cylindrical shells with a constant thickness by using the first order shear deformation theory (FSDT) and solved them by applying the perturbation method. The buckling load of a cylindrical shell with a variable thickness was presented analytically by Koiter et al. [5]. The governing equations were determined by considering the classical shell theory (CST) with the linear kinematic relations, and they were solved using the asymptotic expansion. Li et al. [6] obtained the axial buckling load of a composite shell with a variable thickness by using the finite difference method. The thickness varied sinusoidally and the kinematic relations were linear. Andrianov et al. [7] determined the buckling load of a shell with a circumferential reinforcing band under external pressure. The shell was divided into several parts with constant thicknesses and each part was solved separately and the buckling load was determined by considering the continuity conditions. Gusic et al. [8] studied the effects of circumferential changes of the thickness on the buckling load. The governing equations were derived by considering the von-Karman theory and the solution was obtained with the finite elements (FE) method. Sofiyev and Erdem [9]

investigated the stability of a heterogeneous cylindrical shell with a variable thickness under uniform external pressure. The stability equations were derived by using the linear kinematic relations and modified Donnell's theory. Filippov et al. [10] obtained the buckling load and natural frequencies of a cylindrical shell with a variable thickness and curvilinear edge. The governing equations were extracted by considering linear kinematic relations and they were solved by using the matched asymptotic solution and FE method. Aghajari et al. [11] studied the buckling and post-buckling behavior of a cylindrical shell with a variable thickness by using the experimental and numerical methods. Luong and Hoach [12] determined the buckling load of a cylindrical panel with a variable thickness by using the Galerkin method. The governing equations were obtained linearly by considering the small deformation assumption. Luong et al. [13] investigated the buckling behavior of a cylindrical shell with a variable thickness under external pressure. The kinematic relations were linear and the governing equations for the elastic case were solved using the perturbation technique and Bubnov-Galerkin method. Fakhim et al. [14] presented the buckling load of a shell with a variable thickness under the hydrostatic pressure, experimentally. The thickness profile changed stepwise and the shell had a conical cap. The buckling load of a shell with a stepwise variable thickness was calculated by Chen et al. [15]. They predicted the buckling load by using the weighted smeared wall method. Chen et al. [16] solved the Koiter equations and obtained the buckling load of a shell with a stepwise variable thickness. The solution was determined by using the perturbation technique for each part of the shell with a constant thickness. Shariyat and Asgari [17] extracted the equation of a nonhomogeneous and temperature dependent shell with variable thickness by considering

Corresponding author, E-mail: hamidre_2000@yahoo.com

the third-order shear deformation theory and nonlinear von-Karman assumptions and determined the buckling temperature by using the FE method. Alashti and Ahmadi [18] investigated the buckling of a cylindrical panel with a varying thickness. The governing equations were obtained by considering the linear kinematic relations and these equations were solved by differential quadrature (DQ) method. Fan et al. [19] introduced an analytical method for dynamic buckling load determination of the shell with a variable thickness. By combining the Fourier series expansion and the perturbation technique, analytical formulas for buckling load of cylindrical shells with a variable thickness under time-dependent external pressure were determined. They converted the shell to some cylinders with constant thicknesses. Zhou et al. [20] presented an analytical method to investigate the buckling behavior of the shell with a stepwise variable thickness under uniform external pressure. The analytical method consists of separation of variables method, perturbation technique, and Fourier series expansion. The presented method is just suitable for the shells with a stepwise thickness.

To determine the buckling load of the shells with a variable thickness, most authors have used the numerical methods. Some of them have used the analytical methods based on the approximated functions, e.g., Frobenius series. The analytical methods were usually used for the linear problems and the classical shell theories. In this article, an analytical procedure is presented to determine the buckling load of an axisymmetric shell with a variable thickness. The displacement field is defined using the FSDT. The kinematics of the shell obeys the nonlinear von-Karman relations and the Hooke's law is used as the constitutive equation. The governing equations, which are a system of nonlinear coupled differential equations with variable coefficients, are solved analytically using the perturbation technique. The analytical results are compared with the FE method and other available works.

2- Governing Equations

The horizontal and vertical coordinates of a point on the longitudinal section of an axisymmetric cylinder with a varying thickness are defined by r and x , respectively (Fig. 1) and $r=R(x)+z$; $R(x)$ is the middle surface radius and z is measured from the middle surface. L is the length of the shell and $h(x)=R_{outer}-R_{inner}(x)$. By considering the FSDT, the displacement field in the axisymmetric case is assumed as:

$$\begin{aligned} U_x(x, z) &= u_0(x) + zu_1(x) \\ U_z(x, z) &= w_0(x) + zw_1(x) \end{aligned} \quad (1)$$

U_z and U_x are the radial and axial displacements, respectively, u_0 and w_0 are the middle surface displacements. u_0 , u_1 , w_0 and w_1 are unknown functions of x . By considering the von-Karman kinetic relations, the strain-displacement relations are [21]:

$$\begin{aligned} \varepsilon_{xx} &= \frac{\partial U_x}{\partial x} + \frac{1}{2} \left(\frac{\partial U_z}{\partial x} \right)^2 \\ \varepsilon_{\theta\theta} &= \frac{U_z}{r}; \quad \varepsilon_{zz} = \frac{\partial U_z}{\partial z} + \frac{1}{2} \left(\frac{\partial U_z}{\partial z} \right)^2 \\ \gamma_{xz} &= \frac{\partial U_x}{\partial z} + \frac{\partial U_z}{\partial x} + \frac{\partial U_x}{\partial x} \frac{\partial U_z}{\partial z} \end{aligned} \quad (2)$$

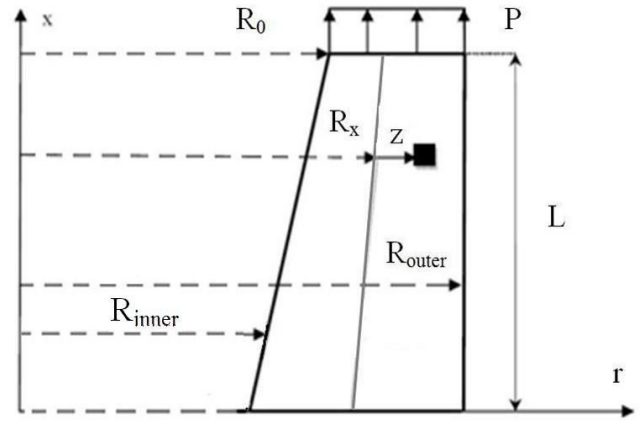


Fig. 1. Longitudinal section of shell subjected to axial stress at $x=L$

For FSDT, the normal transverse strain is constant in z -direction but in the CST, it equates to zero. The Hooke's law for a homogeneous, isotropic and linear elastic material is as follows;

$$\begin{aligned} U_x(x, z) &= u_0(x) + zu_1(x) \\ U_z(x, z) &= w_0(x) + zw_1(x) \end{aligned} \quad (3)$$

Where λ and μ are lame's constants and $A=\lambda+2\mu$. The governing equations can be derived using the principle of virtual work which states that $\delta U = \delta W$. U is the strain energy and W is the potential energy due to in-plane load. We have [22]:

$$U = \iiint \frac{1}{2} (\sigma_x \varepsilon_x + \sigma_\theta \varepsilon_\theta + \sigma_z \varepsilon_z + \tau_{xz} \gamma_{xz}) dV \quad (4a)$$

$$dV = (R(x) + z) dx \cdot dz \cdot d\theta$$

$$W_p = \frac{1}{2} \iiint -P \left(\frac{\partial U_z}{\partial x} \right)^2 dV, \quad 0 \leq x \leq L \quad (4b)$$

$$0 \leq \theta \leq 2\pi, \quad -h(x)/2 \leq z \leq h(x)/2$$

Where P (N/m²) is stress at $x=L$. The stress resultants are defined as:

$$\begin{aligned} \{N_x, M_x, P_x\} &= \int_{-h/2}^{h/2} \{1, z, z^2\} \sigma_x (1 + z/R) dz \\ \{N_\theta, M_\theta\} &= \int_{-h/2}^{h/2} \{1, z\} \sigma_\theta dz \\ \{Q_x, M_{xz}\} &= \kappa \int_{-h/2}^{h/2} \{1, z\} \tau_{xz} (1 + z/R) dz \\ N_z &= \int_{-h/2}^{h/2} \sigma_z (1 + z/R) dz; \quad R = R(x); h = h(x) \end{aligned} \quad (5)$$

Where, κ is the shear correction factor which is assumed 5/6. By inserting Eqs. (1-3,5) into the principle of virtual work and equating each of the coefficients δu_0 , δu_1 , δw_0 , δw_1 to zero, we obtain the following equations in terms of stress

resultants:

$$\begin{aligned}
 \text{eq1: } & \frac{d}{dx}(RN_x) = 0; \quad \text{eq2: } \frac{d}{dx}(RM_x) - RQ_x = 0; \\
 \text{eq3: } & \frac{d}{dx} \left(RN_x \frac{dw_0}{dx} + RM_x \frac{dw_1}{dx} + RQ_x (1+w_1) \right) \\
 & - N\theta - P \frac{d}{dx} \left(Rh \frac{dw_0}{dx} + \frac{h^3}{12} \frac{dw_1}{dx} \right) = 0 \\
 \text{eq4: } & \frac{d}{dx} \left(RM_x \frac{dw_0}{dx} + RP_x \frac{dw_1}{dx} + RM_{xz} \right) \\
 & - RQ_x \frac{dw_0}{dx} - RN_z (1+w_1) + w_1 \frac{d}{dx} (RM_{xz}) \\
 & - M\theta - P \frac{d}{dx} \left(\frac{h^3}{12} \left(R \frac{dw_1}{dx} + \frac{dw_0}{dx} \right) \right) = 0; \quad h=h(x); \quad R=R(x)
 \end{aligned} \tag{6}$$

By inserting Eqs. (2-3,5) into Eq. (6) the governing equations as a function of displacements are extracted. These equations are a system of four nonlinear coupled differential equations with variable coefficients. The general form of these equations is as follows. L_1 to L_4 are differential operators. The dimensionless form of equations has been reported in the appendix.

$$\text{eq}_1 : L_1 \left[x, \frac{d}{dx}, \left(\frac{d}{dx} \right)^2, u_0, u_1, w_0, w_1, P, R, h \right] = 0 \tag{7a}$$

$$\text{eq}_2 : L_2 \left[x, \frac{d}{dx}, \frac{d^2}{dx^2}, \left(\frac{d}{dx} \right)^2, \frac{d}{dx} \square \frac{d^2}{dx^2}, u_0, u_1, w_0, w_1, R, h \right] = 0 \tag{7b}$$

$$\text{eq}_3 : L_3 \left[x, \frac{d}{dx}, \frac{d^2}{dx^2}, \left(\frac{d}{dx} \right)^2, \frac{d}{dx} \square \frac{d^2}{dx^2}, \left(\frac{d}{dx} \right)^3, u_0, u_1, w_0, w_1 \right] = 0 \tag{7c}$$

$$\text{eq}_4 : L_4 \left[x, \frac{d}{dx}, \frac{d^2}{dx^2}, \left(\frac{d}{dx} \right)^2, \frac{d}{dx} \square \frac{d^2}{dx^2}, \left(\frac{d}{dx} \right)^3, \frac{d}{dx} \square \left(\frac{d}{dx} \right)^3 \right] = 0 \tag{7d}$$

3- Analytical Solution

The perturbation technique is used to solve the governing equations. For this purpose, it is necessary to convert the equation to dimensionless form. We define the following new parameters,

$$\begin{aligned}
 x^* &= \frac{x}{L}; \quad h^* = \frac{h}{h_0}; \quad R^* = \frac{R}{R_0} \\
 u_0^* &= \frac{u_0}{h_0}; \quad w_0^* = \frac{w_0}{h_0}; \quad \varepsilon = \frac{h_0}{L}; \quad V^* = \varepsilon \frac{du_0^*}{dx^*} \\
 P_1^* &= \frac{P}{A}; \quad \theta_1 = \frac{\lambda}{A}; \quad \theta_2 = \frac{\mu}{A}; \quad Z_1 = \frac{L}{R_0}; \\
 m &= \ln \frac{2R+h}{2R-h}
 \end{aligned} \tag{8}$$

Where h_0 and R_0 are the thickness and radius characteristics, respectively (the thickness and radius at $x^*=1$ as shown in Fig.1) and (*) stands for a dimensionless quantity. ε is a small parameter which will be taken as the perturbation parameter. By using Eqs. (7-8) and considering the new variable $\eta=x^*/\varepsilon$, the governing equations are converted to the dimensionless form. In order to solve them, the straightforward expansion method has been used [23]. This solution is considered as a uniform expansion of ε .

$$\begin{Bmatrix} V^* \\ u_1^* \\ w_0^* \\ w_1^* \end{Bmatrix} = \varepsilon \begin{Bmatrix} V_0^* \\ u_{10}^* \\ w_{00}^* \\ w_{10}^* \end{Bmatrix} + \varepsilon^2 \begin{Bmatrix} V_1^* \\ u_{11}^* \\ w_{01}^* \\ w_{11}^* \end{Bmatrix} \tag{9}$$

The Taylor expansions of the middle surface radius and thickness about $\varepsilon=0$ are as follows:

$$\begin{aligned}
 R^*(x^*) &= R^*(0) + \varepsilon \eta \left. \frac{dR^*}{dx^*} \right|_{x^*=0} + \dots \\
 h^* &= h^*(0) + \varepsilon \eta \left. \frac{dh^*}{dx^*} \right|_{x^*=0} + \dots
 \end{aligned} \tag{10}$$

By inserting Eqs. (9) and (10) into the dimensionless form of equations, the equations of the same order of ε are determined. The order-one equations are as Eq. (11). The higher orders of these equations do not provide any new information about the buckling load and they can just improve the buckling mode shape of the shell.

$$\begin{aligned}
 \text{eq1: } & \left(R^* h^* (\theta_1 w_{10}^* + V_0^*) \right)' = 0 \\
 \text{eq2: } & -12\kappa\theta_2 R^* (u_{10}^* + w_{00}^*) \\
 & + h^{*2} (R^* u_{10}^{*'}) + 3R^* h^* h^{*'} u_{10}^{*'} = 0 \\
 \text{eq3: } & \kappa\theta_2 R^{*2} (h^* w_{00}^{*'} + h^* u_{10}^{*'}) + \kappa\theta_2 (R^{*2} h^{*'})' u_{10}^* \\
 & - h^* (P_1^* - \kappa\theta_2) (R^{*2} w_{00}^{*'})' - P_1^* R^{*2} h^* w_{00}^{*'} = 0 \\
 \text{eq4: } & \left(-\frac{h^{*2}}{12} (w_{10}^* R^*)' - \frac{1}{4} w_{10}^* h^* h^{*'} R^* \right) (P_1^* - \kappa\theta_2) \\
 & - R^* w_{10}^* - \theta_1 R^* V_0^* = 0
 \end{aligned} \tag{11}$$

where $()' = d/d\eta$, $()'' = d^2/d\eta^2$. Eq. (11) is a system of homogeneous coupled ordinary differential equations with constant coefficients which have the exact solution. The solution of Eq. (11) is considered as in the following:

$$\{V_0^*, u_{10}^*, w_{00}^*, w_{10}^*\} = \{v_1, v_2, v_3, v_4\} \exp(m\eta) \tag{12}$$

By inserting Eq. (12) into Eq. (11), we have:

$$[ax]_{4 \times 4} \{v_1, v_2, v_3, v_4\}^T = \{0\}_{4 \times 1} \tag{13}$$

For a nontrivial solution, we set the determinant of Eq. (13)

to zero. The roots of this algebraic equation are $m_1, m_2, m_3, m_4, m_5, m_6$ which are functions of P^* . Thus, the general solution is:

$$\begin{Bmatrix} V_0^* \\ u_{10}^* \\ w_{00}^* \\ w_{10}^* \end{Bmatrix}^T = \sum_{i=1}^6 C_i \{V\}_i \exp(m_i \eta) \tag{14}$$

$$\{V\}_i = \{v_1, v_2, v_3, v_4\}_{m=m_i}^T ; i = 1..6$$

The constants C_i are determined from the boundary conditions which are clamped at $x^*=0$ and at $x^*=1$, it is $u_{10}^*=w_{10}^*=w_{00}^*=0$. By applying the boundary conditions, we have $[bx]_{6 \times 6} \{C_1, C_2, C_3, C_4, C_5, C_6\}^T = \{0\}_{6 \times 1}$. For a nontrivial solution, the determinant of matrix coefficients is equated to zero. It is a complicated algebraic function in terms of P_1^* . The roots of this equation which are calculated by using the bisection method are the dimensionless buckling load.

4- Numerical Analysis

ANSYS 11 FE package has been used for the buckling analysis of the cylindrical shells with a varying thickness. PLANE82 element in axisymmetric mode, which is an element with eight nodes and two translational degrees of freedom at each node, was used for the buckling analysis. This element is an axisymmetric element and is used to model the longitudinal section of the cylinder. The shell is clamped at $x^*=0$ and at the section $x^*=1$ it is restricted to move in the radial direction. The shell properties have been listed in Table 1. For the shell with a variable thickness, the inner radius has linear and nonlinear variations and the outer radius is constant in the case studies. Fig. 2 shows the selected element, mesh pattern, loading, boundary conditions and buckled shell.

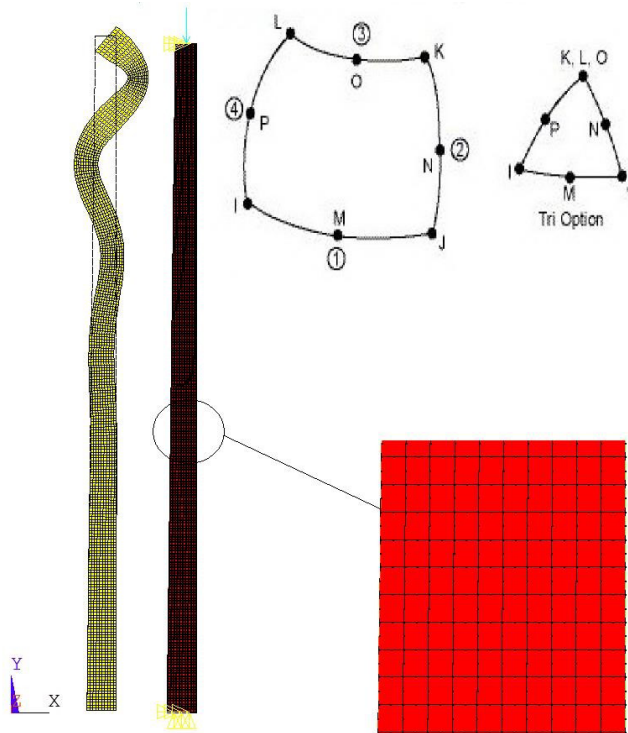


Fig. 2. Mesh pattern and buckled shell.

Table 1. Shell characteristics

Property	Value
Shell length	$L=0.8$ m
Young's modulus	$E=200$ GPa
Poisson's ratio	$\nu=0.3$

5- Results and Discussion

According to the mentioned formulation, the buckling load of a shell with a variable thickness has been determined analytically. A program has been prepared to perform the calculations using MAPLE13 mathematical software. The dimensionless buckling load of shells with different thicknesses have been reported in Table 2. It is seen that the increase of the thickness decreases the difference percentage and the analytical results are improved by increasing the thickness. In other words, the current method is more useful for thicker shells (Fig. 3).

Table 2. Dimensionless buckling load of various shells with Rinner($x^*=0$)=0.14m, Rinner($x^*=1$)=0.15m

Router (m)	FE	Analytical	Difference percentage with respect to FE
0.154	0.0209	0.0203	2.8%
0.156	0.0297	0.0260	12.4%
0.158	0.0380	0.0367	3.4%
0.16	0.0472	0.0460	2.5%
0.165	0.0642	0.0604	6%
0.17	0.0810	0.0780	3.6%
0.175	0.0960	0.0953	0.8%

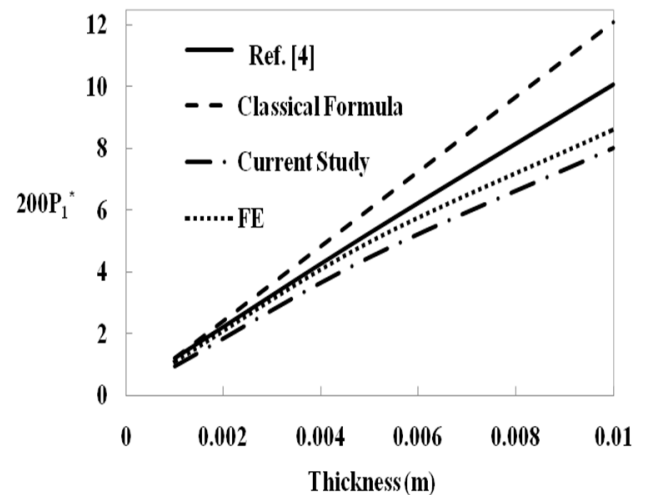


Fig. 3. Effect of thickness on buckling load for the shells with constant thickness – Comparison with classical formula, FE and Ref. [4].

Fig. 3 shows the effect of thickness on the buckling load of the shell with a constant thickness. The results of this study have been compared with those obtained by FE method, the classical (Lorenz) formula [24] and the analytical method which have been presented in reference [4]. Ref. [4] assumes that the radial displacement is independent of z i.e $w_1=0$ (in Eq. (1)). In comparison with the FE method, it has the better

results with respect to our work for smaller thicknesses but when the thickness increases, the presented formulation is closer than to the FE results with respect to Ref. [4]. In other words, for the thicker shells, it is necessary to consider w_1 in Eq. (1). Also, for thin shells, the CST is sufficient to calculate the buckling load.

Fig. 4 shows the buckling load with different inner wall slopes as $R_{inner} = \alpha x^* + R_{inner}(0)$. In all cases, the shells have the same volume. The outer radius is constant. It is seen that by increasing the inner wall slope, the buckling load decreases. Fig. 5 shows the effect of R_m/h_m (which R_m, h_m are the mid-surface radius and thickness of the shell at $x^*=0.5$) on the buckling load. The inner and outer radiuses ranges for Fig. 5 have been reported in Table 3.

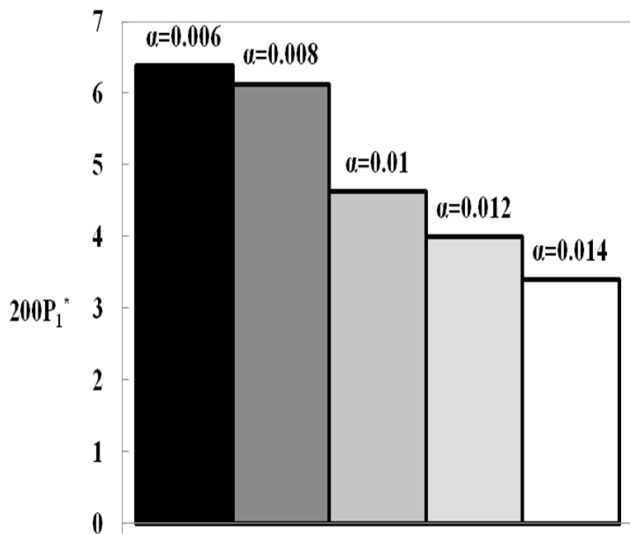


Fig. 4. Buckling load for different slops with $R_{outer} = 0.145m$ (with the same volume).

Table 3. Inner and outer radiuses values in Fig. 4

	Min.	Max.
R_{outer}	0.11m	0.17m
Inner($x^*=0$)	0.8m	0.14m
Inner($x^*=1$)	0.9m	0.15m

It is seen that the buckling load decreases by increasing R_m/h_m ratio. This graph can be approximated as $P_1^* = 123.7(h_m/R_m)^{1.13}$. In CST, the buckling load is proportional to h/R .

In Fig. 6, the buckling load for shells with linear and nonlinear profiles versus different outer radius has been presented. For the linear case, $R_{inner} = 0.01x^* + 0.14$ and for the nonlinear case, $R_{inner} = 0.06x^{*2} - 0.06x^* + 0.155$. In all cases, the shells have the same volume. It is specified that the shells with nonlinear profile have a higher buckling load and, as a result, they can be more efficient.

6- Conclusion

An analytical procedure based on the *FSDT* and the perturbation technique was presented to determine the buckling load of cylindrical shells with a variable thickness.

- This method converts the nonlinear equations with variable coefficients to a system of ordinary differential

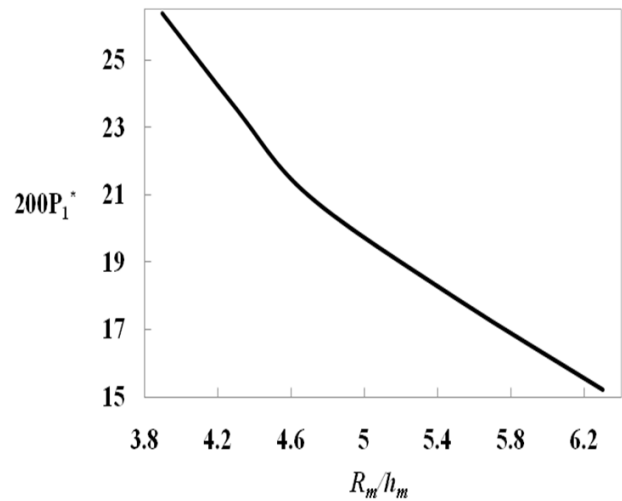


Fig. 5. Effect of R_m/h_m on buckling load.

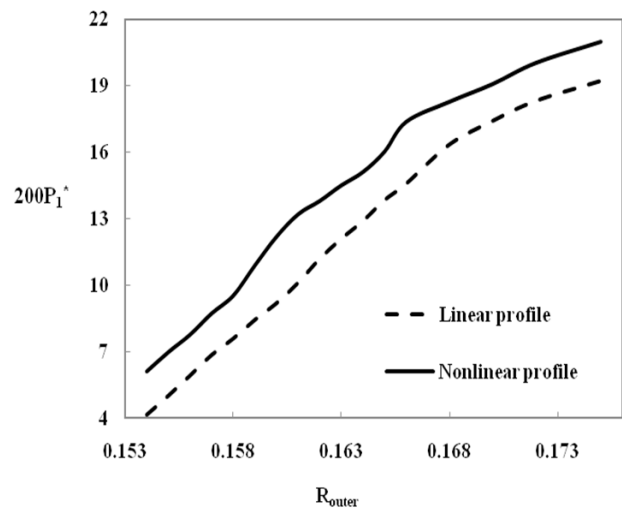


Fig. 6. Buckling load for linear and nonlinear variation of shell profile.

equations with constant coefficients. This system of equations has closed-form solutions.

- This analytical solution has a fast convergence and good accuracy.
- This analysis does not require to build the *FE* models and mesh them.
- The geometrical properties (inner and outer radius and the shell length), are just as an input for the prepared program. Thus, one can perform the sensitivity analysis easily for different shells with linear and nonlinear thickness variations.
- By using the *FSDT*, the difference between analytical and *FE* results for thicker shells decreases.
- For the cylindrical shells with a linear thickness variation, by increasing the gradient of the inner profile, the buckling load decreases.
- By increasing R_m/h_m in cylindrical shells with variable thickness, the buckling load decreases significantly.
- The presented method is capable of determining the buckling load for the shells with an arbitrary continuous

profile (linear or nonlinear).

- The shells with the nonlinear profiles have a higher efficiency in comparison with the shells with linear profiles for the same volume.
- According to the FSDT, the buckling load of shells is proportional to $(h_m/R_m)^{1,13}$, which for the CST, it is proportional to h_m/R_m .
- Considering w_1 in Eq. (1), improves the results especially for the thicker shells.

Appendix

$$eq1 : (\theta Z_1 (w_0^* h^*)' + (\frac{h^*3 Z_1}{12} (w_1^* w_0^* + u_1^*)))' \epsilon + \frac{1}{2} (R^* h^* (w_0^*)^2 + (w_1^*)^2)' + (R^* h^* (V^* + \theta w_1^*))' + \frac{1}{24} (R^* h^*3 (w_1^*)^2)' = 0$$

$$eq2 : (\frac{1}{4} h^* h^* V^* + \frac{1}{32} h^*3 h^* (w_1^*)^2 + \frac{1}{8} h^* h^* (w_0^*)^2 + \frac{1}{12} h^*2 w_0^* w_0^* + \frac{1}{80} h^*4 w_1^* w_1^* + \frac{1}{6} h^*2 \theta w_1^* + \frac{1}{12} h^*2 \theta w_1^* w_1^* - \frac{1}{10} \kappa h^*2 \theta (w_1^* + w_1^*) + \frac{1}{12} h^*2 V^* + \frac{1}{8} h^* h^* \theta (4w_1^* + w_1^*)) h^* Z_1 \epsilon + ((\frac{1}{12} h^*2 R^* + \frac{1}{4} h^* h^* R^*) (u_1^* + w_0^* w_1^*)) + \frac{1}{12} h^*2 R^* (w_0^* w_1^* + u_1^* + w_1^* w_0^*) - \frac{6}{5} \kappa \theta_2 R^* (u_1^* + w_0^* w_1^* + w_0^*) h^* = 0$$

$$eq3 : -h^* Z_1^2 w_0^* \epsilon^2 + (2h^* R^* \theta_1 (w_0^*)^2 - 2V^* - 2w_1^* - (w_1^*)^2) + R^* h^*3 (w_1^*)^2 (\frac{1}{5} \kappa \theta_2 (1+w_1^*) + \frac{1}{8} \theta_1 + \frac{1}{12} \theta w_1^*) + \frac{1}{4} h^* R^* h^*2 (w_1^* (V^* - P_1^* + \frac{3}{2} (w_0^*)^2) + \frac{6}{5} \kappa \theta_2 w_1^* (1+w_1^*)) + \frac{\theta_1 w_1^* (4+w_1^*)}{2} + \frac{6}{5} \kappa \theta_2 (w_0^* (u_1^*)) + h^* R^* \theta w_1^* w_0^* + \frac{1}{32} h^* R^* h^*4 (w_1^*)^3 + \frac{1}{12} R^* h^*3 (w_1^* V^* + 3w_1^* w_0^* w_1^*) + w_0^* u_1^* + w_1^* (-P_1^* + 1 + V^* + 2w_1^* \theta + \frac{w_1^*2 \theta_1}{2} + \frac{6}{5} \kappa w_1^*2 \theta_2 + \frac{12}{5} \kappa w_1^* \theta) + \frac{3}{2} (w_0^*)^2 w_1^* + w_0^* u_1^* + h^* R^* \theta w_1^* w_0^* + \frac{3}{160} R^* h^*5 (w_1^*)^2 w_1^* Z_1 \epsilon + R^* h^*2 (2w_0^* w_1^* - w_0^* P_1^*) + \frac{1}{2} (w_0^*)^3 + u_1^* w_1^* + w_0^* V^* + \frac{1}{2} \theta w_1^* (w_1^*)^2 + \theta w_1^* w_1^* + h^* R^*2 w_0^* w_1^* (\theta + \frac{12}{5} \kappa \theta_2 + \theta w_1^*) - h^* R^* R^* (w_0^* P_1^* - \frac{6}{5} \kappa \theta_2 (u_1^* + w_0^*)) - \frac{1}{2} (w_0^*)^3 + \frac{6}{5} \kappa \theta_2 R^*2 h^* w_0^* ((w_1^*)^2 + 1) + \frac{6}{5} \kappa \theta_2 R^*2 h^* (w_1^* u_1^*) + \frac{1}{12} R^* h^*3 R^* w_1^* u_1^* + \frac{1}{8} R^* h^*3 R^* w_0^* (w_1^*)^2 + \frac{3}{8} R^*2 h^* h^*2 w_0^* (w_1^*)^2 + h^* R^* R^* w_0^* (V^* + \theta w_1^* + \frac{12}{5} \kappa \theta_2 w_1^* + \frac{6}{5} \kappa \theta_2 w_1^*2 + \frac{\theta_1 w_1^*2}{2})$$

$$+ \frac{12}{5} \kappa R^*2 h^* \theta w_0^* w_1^* + \frac{6}{5} \kappa h^* R^* R^* \theta u_1^* w_1^* + R^*2 h^* u_1^* + R^*2 h^* w_0^* (\frac{3}{2} (w_0^*)^2 + \frac{6}{5} \kappa \theta_2 - P_1^* + V^* + 2w_1^* + (w_1^*)^2) + \theta w_1^* + \frac{1}{2} \theta (w_1^*)^2 + \frac{1}{4} R^*2 h^* h^*2 u_1^* w_1^* + R^*2 h^* (w_0^* V^* + \frac{6}{5} \kappa \theta_2 u_1^*) + R^*2 h^*3 (\frac{1}{12} (u_1^* w_1^*)' + \frac{1}{8} (w_1^*)^2 w_0^*) + \frac{1}{4} w_0^* w_1^* w_1^* = 0$$

$$eq4 : (\frac{1}{12} h^*2 (u_1^* w_1^* (\frac{6}{5} \kappa \theta_2 - \theta) + \theta w_0^* w_1^* + (w_0^* V^*)' + \theta w_0^* w_1^*) + 2w_1^* w_0^* (\frac{6}{5} \kappa \theta_2 + \theta) + \frac{1}{2} w_0^* (w_1^*)^2 (\theta_1 + \frac{12}{5} \kappa \theta_2) - w_0^* (P_1^* - \frac{6}{5} \kappa \theta_2) + u_1^* (\frac{6}{5} \kappa \theta_2 - 2\theta)) - \theta w_0^* w_1^* + \frac{1}{4} h^* h^* (\frac{6}{5} \kappa \theta_2 (u_1^* + w_0^*) + \frac{1}{2} (w_0^*)^3) - w_0^* P_1^* + w_0^* V^* + \theta w_1^* w_0^* + \frac{6}{5} \kappa \theta_2 w_1^* ((u_1^* + w_0^*) + 2w_0^*) + \frac{1}{2} \theta w_1^* ((w_1^*)^2 + 4w_1^*) + \frac{1}{16} h^*3 h^* (u_1^* w_1^* + \frac{3}{2} w_0^* (w_1^*)^2) - \theta w_1^* + \frac{1}{80} h^*4 ((w_1^* u_1^*)' + \frac{3}{2} w_1^* w_0^* + 3w_0^* w_1^* w_1^*) + \frac{1}{8} h^*2 (w_0^*)^2 w_0^* Z_1 \epsilon + \frac{1}{4} h^* h^* R^* (w_1^* ((\frac{6}{5} \kappa \theta_2 - P_1^*) + V^* + \frac{6}{5} \kappa \theta_2 (w_1^*)^2) + \theta w_1^* + \frac{\theta_1 (w_1^*)^2}{2} + \frac{12}{5} \kappa \theta_2 w_1^* + \frac{3(w_0^*)^2}{2}) + u_1^* w_0^* + \frac{1}{160} h^*4 R^* (w_1^*)^3 - \frac{6}{5} \kappa R^* \theta w_0^* u_1^* - R^* \theta w_1^* (V^* + \frac{1}{2} (w_0^*)^2) + \frac{1}{12} h^*2 R^* ((u_1^* w_0^*)' + \frac{3}{2} (w_0^*)^2 w_1^* + \frac{1}{2} (w_1^*)^2 (\theta_1 + \frac{12}{5} \kappa \theta_2)) + w_1^* (V^* + \frac{6}{5} \kappa \theta_2 (2w_1^* + (w_1^*)^2 + 1) + \theta w_1^* + \frac{\theta_1 (w_1^*)^2}{2} - P_1^*) + 3w_0^* w_1^* w_0^* + w_1^* V^* + w_1^* (w_1^*)^2 (\frac{6}{5} \kappa \theta_2 + \frac{\theta_1}{2}) - R^* (\theta V^* + \frac{1}{2} (w_1^*)^3 + (w_0^*)^2 (\frac{6}{5} \kappa \theta_2 + \frac{6}{5} \kappa \theta_2 w_1^* + \frac{1}{2}) + \frac{3}{2} (w_1^*)^2 + w_1^*) + \frac{1}{12} h^*2 R^* (w_0^* u_1^* - w_1^* (P_1^* - \frac{6}{5} \kappa \theta_2) + \frac{3}{2} w_1^* (w_0^*)^2) + w_1^* (V^* + \theta w_1^* + \frac{12}{5} \kappa \theta_2 w_1^* + \frac{\theta_1 (w_1^*)^2}{2} + \frac{6}{5} \kappa \theta_2 (w_1^*)^2) + \frac{1}{32} h^*3 h^* R^* (w_1^*)^3 + \frac{3}{160} h^*4 R^* (w_1^*)^2 w_1^* = 0$$

References

- [1] J. Hutchinson, Axial buckling of pressurized imperfect cylindrical shells, *AIAA J*, 3(8) (1965) 1461-1466.
- [2] V. Weingarten, E. Morgan, P. Seide, Elastic stability of thin-walled cylindrical and conical shells under axial compression, *AIAA J*, 3(3) (1965) 500-505.
- [3] Z. Malik, J. Morton, C. Ruiz, An experimental investigation into the buckling of cylindrical shells of variable-wall thickness under radial external pressure, *Experimental Mechanics*, 19(3) (1979) 87-92.
- [4] F. Mahboubi Nasrekani, H. Eipakchi, Elastic buckling of axisymmetric cylindrical shells under axial load using first order shear deformation theory, *ZAMM-Journal of Applied Mathematics and Mechanics/Zeitschrift für Angewandte Mathematik und Mechanik*, 92(11-12) (2012) 937-944.
- [5] W. Koiter, I. Elishakoff, Y. Li, J. Starnes, Buckling of an axially compressed cylindrical shell of variable thickness, *International Journal of Solids and Structures*, 31(6) (1994) 797-805.

- [6] Y. Li, I. Elishakoff, J. Starnes, Axial buckling of composite cylindrical shells with periodic thickness variation, *Computers & structures*, 56(1) (1995) 65-74.
- [7] I. Andrianov, B. Ismagulov, M. Matyash, Buckling of cylindrical shells of variable thickness, loaded by external uniform pressure, *Tech. Mech*, 20(4) (2000) 349-354.
- [8] G. Gusic, A. Combescure, J. Jullien, The influence of circumferential thickness variations on the buckling of cylindrical shells under external pressure, *Computers & Structures*, 74(4) (2000) 461-477.
- [9] A.H. Sofiyev, H. Erdem, The stability of non-homogeneous elastic cylindrical thin shells with variable thickness under a dynamic external pressure, *Turkish Journal of Engineering and Environmental Sciences*, 26(2) (2002) 155-166.
- [10] S. Filippov, D. Ivanov, N. Naumova, Free vibrations and buckling of a thin cylindrical shell of variable thickness with curve linear edge, *Technische Mechanik*, 25(1) (2005) 1-8.
- [11] S. Aghajari, K. Abedi, H. Showkati, Buckling and post-buckling behavior of thin-walled cylindrical steel shells with varying thickness subjected to uniform external pressure, *Thin-walled structures*, 44(8) (2006) 904-909.
- [12] N.T.H. Luong, T.S.S. Hoach, Stability of cylindrical panel with variable thickness, *Vietnam Journal of Mechanics*, 28(1) (2006) 56-65.
- [13] H.L.T. Nguyen, I. Elishakoff, V.T. Nguyen, Buckling under the external pressure of cylindrical shells with variable thickness, *International Journal of Solids and Structures*, 46(24) (2009) 4163-4168.
- [14] Y. Fakhim, H. Showkati, K. Abedi, Experimental study on the buckling and post-buckling behavior of thin-walled cylindrical shells with varying thickness under hydrostatic pressure, in: *Proceedings of the international association for shell and spatial structures (IASS) symposium*, 2009.
- [15] L. Chen, J.M. Rotter, C. Doerich, Buckling of cylindrical shells with stepwise variable wall thickness under uniform external pressure, *Engineering Structures*, 33(12) (2011) 3570-3578.
- [16] Z. Chen, L. Yang, G. Cao, W. Guo, Buckling of the axially compressed cylindrical shells with arbitrary axisymmetric thickness variation, *Thin-Walled Structures*, 60 (2012) 38-45.
- [17] M. Shariyat, D. Asgari, Nonlinear thermal buckling and postbuckling analyses of imperfect variable thickness temperature-dependent bidirectional functionally graded cylindrical shells, *International Journal of Pressure Vessels and Piping*, 111 (2013) 310-320.
- [18] R.A. Alashti, S.A. Ahmadi, Buckling of imperfect thick cylindrical shells and curved panels with different boundary conditions under external pressure, *Journal of Theoretical and Applied Mechanics*, 52 (2014) 25-36.
- [19] H.-G. Fan, Z.-P. Chen, W.-Z. Feng, F. Zhou, G.-W. Cao, Dynamic buckling of cylindrical shells with arbitrary axisymmetric thickness variation under time dependent external pressure, *International Journal of Structural Stability and Dynamics*, 15(03) (2015) 1450053.
- [20] F. Zhou, Z. Chen, H. Fan, S. Huang, Analytical study on the buckling of cylindrical shells with stepwise variable thickness subjected to uniform external pressure, *Mechanics of Advanced Materials and Structures*, 23(10) (2016) 1207-1215.
- [21] M. Amabili, *Nonlinear vibrations and stability of shells and plates*, Cambridge University Press, New York, 2008.
- [22] X. Xu, J. Ma, C.W. Lim, H. Chu, Dynamic local and global buckling of cylindrical shells under axial impact, *Engineering Structures*, 31(5) (2009) 1132-1140.
- [23] A.H. Nayfeh, *Introduction to perturbation techniques*, John Wiley & Sons, New York, 1981.
- [24] S. Timoshenko, *Theory of elastic stability*, 2 ed., McGraw-Hill, New York, 1963.

Please cite this article using:

F. Mahboubi Nasrekani and H. R. Eipakchi, An Analytical Procedure for Buckling Load Determination of an Axisymmetric Cylinder with Non-Uniform Thickness Using Shear Deformation Theory, *AUT J. Mech. Eng.*, 1(2) (2017) 211-218.

DOI: 10.22060/mej.2017.12557.5364



